IOP Conference Series: Materials Science and Engineering

PAPER • OPEN ACCESS

Advanced Acoustic Emission Source Location in Aircraft Structural Testing

Advanced Acoustic Emission Source Location in Aircraft Structural Testing

S Grigg, C A Featherston, M Pearson & R Pullin
Cardiff School of Engineering, Cardiff University, Queen's Buildings, The Parade, Cardiff, CF24 3AA

Abstract. Acoustic emission (AE) is an in situ Structural Health Monitoring (SHM) technique, where a structure is monitored for the ultrasonic waves produced due to crack growth. A major challenge with AE when applied to aircraft, and other complex structures, is that wave propagation is significantly affected by stiffeners, holes, thickness changes and other complexity. This reduces the accuracy of traditional source location techniques, that are based on a singular propagating wave speed. The Delta-T method enables higher levels of accuracy by mapping the structure and accounting for these changes. In this work AE monitoring equipment was installed on a section of an aluminium Airbus A320 wing. Location trials showed the Delta-T technique improved the average error from 85mm to 23mm, for artificial Hsu-Nielson sources, compared to the commercial standard technique. Testing under fatigue however demonstrated the challenges encountered when inspecting 3D structures (due to multiple signal paths) with significant levels of background noise. Of two cracks identified in the structure, the first of these was successfully detected and located, whilst the other was missed due to high machine noise and unrepresentative loading.

1. Introduction

Many aircraft structures, such as much of the wing, are designed to be damage tolerant; this ensures that any damage within the structure is detected significantly before any failure occurs. Prior to flight all aircraft undergo substantial testing of components and entire airframes, in both static and fatigue tests, to ensure failure will not occur in service. Problems do still occur however, such as the accidental finding of cracks on the rib feet of the Airbus A380 (Kaminski-Morrow, 2012). In addition to substantial testing prior to commercial flights, aircraft undergo regular inspections. Some of these are quick, visual inspections, however others require the aircraft to be taken out of service for weeks, allowing a thorough inspection of the entire airframe. This costs the operator, both in terms of the cost of Maintenance, Repair and Overhaul (MRO) which typically account for 12%-15% of the total operating costs of an aircraft, and the loss of revenue whilst the aircraft is not in service (Rodrigues Vieira and Loures, 2016).

Not only is inspection costly for operators, the inspection during any large-scale structural testing costs aircraft manufacturers greatly. During a full-scale fatigue test, where an aircraft undergoes dummy flight cycles at an accelerated rate, the airframe is periodically stripped down, and every part inspected for damage. If damage is found it is repaired, and identified as a potential problem area, guiding in-service inspection. The manufacturer does not however know at what point this damage occurred, just that it was during the last block of test cycles, which is likely to represent years of aircraft service.

Structural Health Monitoring (SHM) is the process of continually monitoring a structure for the presence of damage, this can be through a range of techniques, including strain and vibration monitoring. SHM is a branch of Non-Destructive Testing (NDT), in which instead of periodic inspection, the structure is monitored through its entire life, without requiring interruption of service. If properly applied to aerospace this could enable a condition rather than time-based inspection, where when damage is identified the area can be inspected and repaired, enabling less regular inspection intervals for both structural testing and in-service aircraft.

Acoustic Emission (AE) monitoring is a SHM technique which enables the detection, localisation, and characterisation of damage in structures, as it occurs. AE is the sudden release of energy produced by the growth of damage. This then propagates as a transient, high frequency elastic wave, through the structure which can be detected with surface mounted piezoelectric sensors. Several sensors enable localisation of the source of the wave, and analysis of the waveform has shown characterization to be possible (Crivelli *et al.*, 2014; McCrory *et al.*, 2015). Although locating a source is possible in complex structures, such as in an aircraft, the effect these complexities have on wave propagation introduces substantial error. This paper presents the results of a fatigue test on a section of aluminium A320 aircraft wing, where AE is been located using the commercial Time of Arrival (TOA) technique and the advanced Delta-T technique developed at Cardiff University (Baxter *et al.*, 2007).

2. Acoustic Emission Source Location

When AE is generated it propagates as a transient, high frequency elastic wave through the structure, in the form of a bulk, Rayleigh or Lamb wave, dependent on the structure's dimensions. Much of an aircraft, including its wings, consists of thin, plate like structures with stiffeners, meaning waves will propagate as Lamb waves (Lamb, 1917).

The detection of the arrival of a Lamb wave by commercial systems is performed using a threshold crossing method, with a pre-trigger, the crossing identifying an arrival time for the wave at each sensor. With three or more sensors these arrival times enable the location of the source through what is known as the TOA method, discussed in detail in the NDT handbook (Miller and Hill, 1987). This approach assumes constant wave velocity, and a direct wave path; in composite structures this is not always the case. Paget et al. (Paget *et al.*, 2003) wrote an algorithm that accounted for direction dependent wave velocities in composites, however this does not account for additional structural complexity. Baxter et al. (Baxter *et al.*, 2007) developed a method known as Delta-T, in which the structure is mapped with Hsu-Nielson (H-N) sources. H-N sources are a mechanical pencil with custom rocker being broken on the surface of a structure, and the ASTM standard for testing sensor bonding (ASTM, 1999). The difference in wave arrival times between each sensor pair is then used to produce maps of the structure and these maps are used to locate sources based on the best fitting location. This approach was shown by Baxter, and subsequent authors (Al-Jumaili *et al.*, 2016; Holford *et al.*, 2017; Pearson *et al.*, 2017), to significantly improve source location in complex structures.

An addition to the Delta-T technique which has improved accuracy further is the use of the Akaike Information Criterion (AIC) to detect the wave arrival. The AIC function is shown in Equation 1, where T is the length of the waveform and t is the point being analysed. This equation compares the classic variance of two vectors, $x(1:t)$ and $x(t:T)$, the data before and after each point in time to find their similarity; the point at which the transition from noise to signal occurs, gives the lowest AIC value. Pearson et al. (Pearson *et al.*, 2017) and Holford et al. (Holford *et al.*, 2017) showed the increased benefit of using this approach. There are however only limited examples of the Delta-T technique being used to locate AE on real aircraft structures under fatigue.

$$AIC(t) = t\log_{10}\big(var(\{x(1:t)\})\big) + (T - t - 1)\log_{10}\big(var(\{x(t:T)\})\big) \quad (1)$$

A brief outline of the Delta-T method is given in the bullet points below, a full description has been published by Pearson et al. (Pearson *et al.*, 2017).

- Identify test area and draw a regular grid over this, then bond the sensors
- Create five H-N sources at each point, acquiring waveforms at each sensor, use AIC to determine arrival times at each sensor
- For each sensor pair find the time of arrival difference, and average for each point of the grid. This allows construction of a map by linear interpolation between points. In the case of four sensors, six maps are produced (1-2, 1-3, 1-4, 2-3, 2-4 and 3-4)

- Acquire test data from trial locations or structural testing. From this, the arrival times and time differences can be found. These are then compared to each map, and the predicted location determined by finding the best fitting solution for all maps.

3. Test Methods

For this test, a 0.5m x 1.38m section of aluminium A320 aircraft wing was cut from a larger unused surplus part. The wing section, shown in Figure 1, includes stiffeners, each with 90 rivets, and a number of holes where ribs would be attached. The thickness of the panel ranges from 6 mm to 9 mm.

Figure 1. A320 aircraft wing panel

Four Mistras Nano-30 sensors, which have a good frequency response from 125 – 750kHz, were bonded onto the inside of the panel, on the skin of the structure between the stiffeners. The four sensors were located in a rectangle 0.5m x 0.3m in the centre of the panel, shown by the diamonds **Figure 2**. On the outside skin of the panel a 1.2m x 0.45m area was mapped (indicated as thin dashed lines in **Figure 2**) with a density of 50mm, a total of 210 points. 20 points were then selected within the mapped area, 18 of these at random and the other two either side of where a hole was later drilled. At each of these points 10 H-N sources were conducted to test the map's accuracy at locating them with both the TOA and Delta-T technique. AE data was collected with a commercial 4 channel Mistras system, with 2/4/6 preamplifiers, set to 40 dB gain.

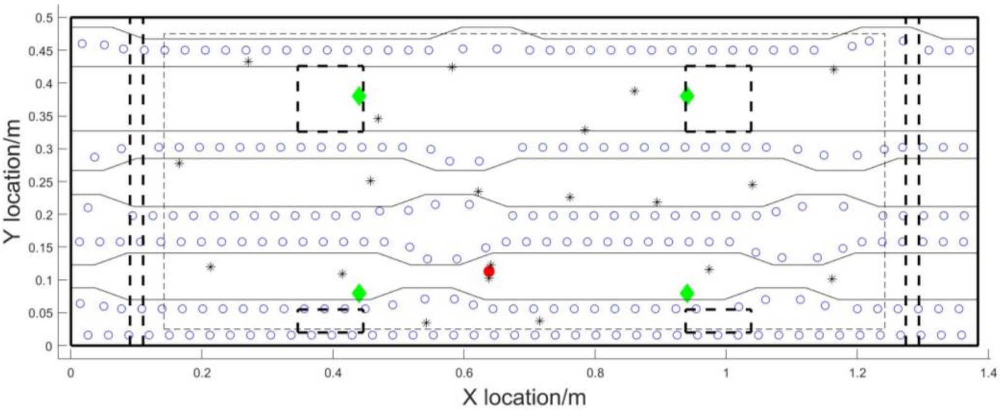

Figure 2. Diagram of A320 aircraft wing panel. Sensor locations shown as diamonds and test locations as '*'. Stiffeners as thin solid lines, the edge of the panel as thick solid lines, mapped area as thin dashed lines and loading points as thick dashed lines. The location of the hole is shown as a filled circle.

A 7mm hole was drilled in the skin of the panel and notched with a hand saw ~4mm each side of the hole in a direction perpendicular to the applied stress. Initial six-point bending fatigue testing was then conducted, this testing put the skin in tension and stiffeners in compression. During this testing a 4mm crack grew from one side of the notch. Test rig noise, due to numerus rubbing test fixtures, meant the no meaningful analysis could be performed on this data.

To reduce the noise the specimen was instead loaded in a four point bend test as shown in Figure 3, the locations of the roller supports and pads on top of the stringers are shown in **Figure 2** as thick dashed lines. Prior to any loading in this configuration a crack was visible from the notch, because of the six-point bend testing. Twenty loading cycles were performed in this configuration, each consisting of between 1,000 and 10,000 cycles. During the first 12 tests the load was gradually increased, up to a max load of 80kN, the remaining tests were always at this load. Between tests, at a 5kN static load, the notch was photographed with a DSLR camera, with a macro lens to identify and track any crack growth.

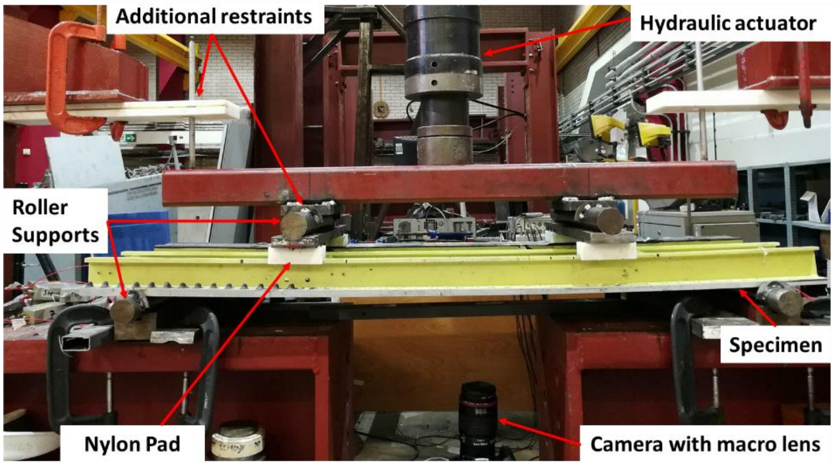

Figure 3. Four-point bend test configuration

4. Results and Discussion

The 20 points tested to trial the Delta-T maps were located in three ways. The simplest of these was the TOA technique used by commercial systems to locate sources, where arrival times were predicted with a threshold crossing approach (45dB threshold). This located with an 85mm average error. TOA was also used combined with AIC predicted arrival times which giving a reduced error of 73mm. Finally, the Delta-T maps were used, which located the sources with an average error of 23mm. **Figure 4** shows the predicted locations for each source.

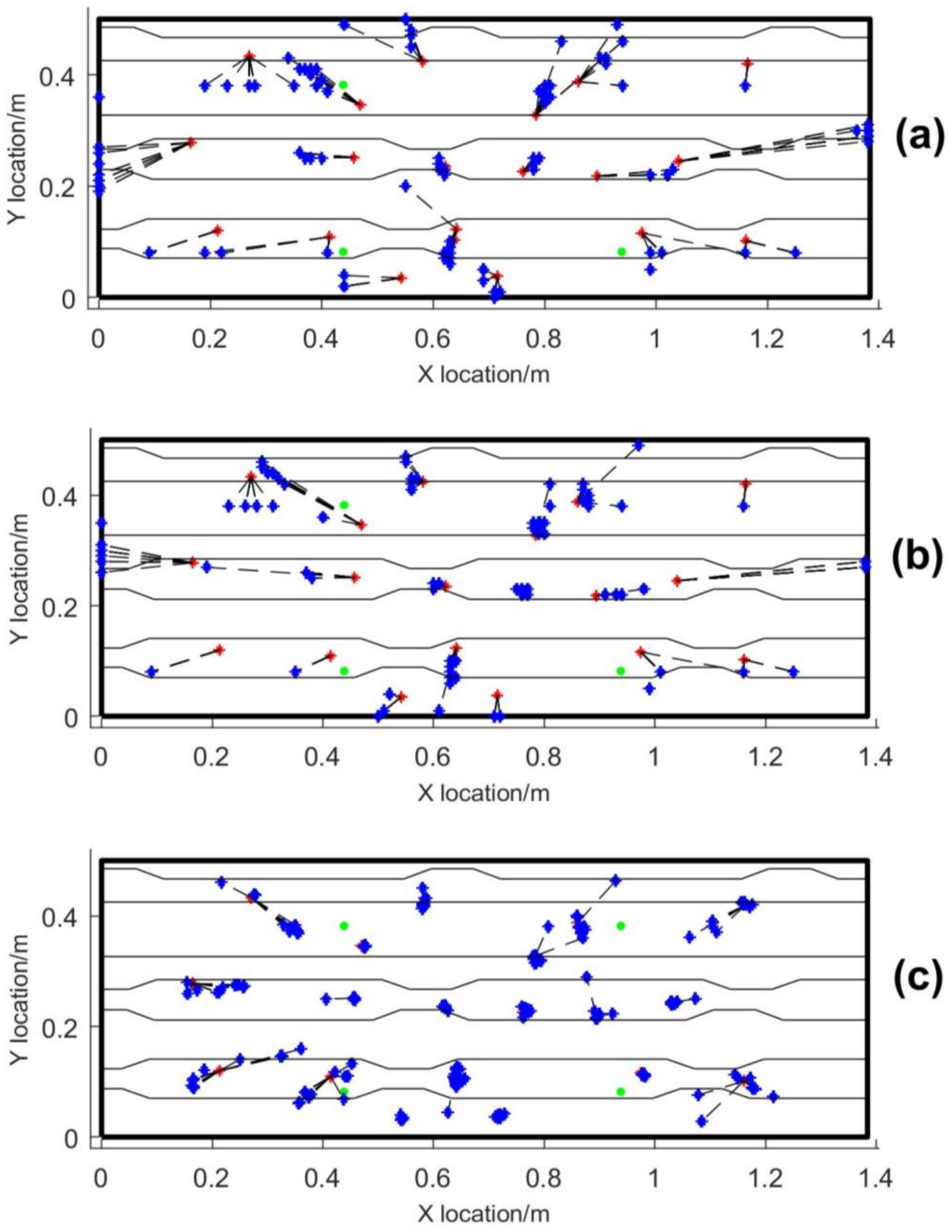

Figure 4. Located sources using TOA with threshold crossing (a), TOA with AIC (b) and Delta-T (c). Test locations shown as red '*' and predicted locations as blue '*'.

The results shown in **Figure 4**, and the average errors seen for each, demonstrate that the Delta-T method was more accurate overall by 50mm. The highest errors for all techniques occurred where the test point is outside of the sensor array; when only considering the eight points within the array, the average errors are 64mm and 55mm for TOA without and with AIC and 10mm for the Delta-T method. For the TOA approach, three sensors are needed for localisation, meaning for data points at the edges/outside the array the waveforms have travelled substantial distances. When travelling in a complex structure waves will have fluctuating velocities, causing increased error. Additionally, signals will have attenuated, reducing the accuracy of the threshold approach, hence the AIC's slightly better accuracy. The lower accuracy for the Delta-T when outside the array is due to a constant time difference for certain sensors when not between the sensors. Being outside the pair means an event which occurs behind one sensor and arrives at another, will appear the same as if the event were at distance from the first. This is shown in the Delta-T map in Figure 5, where the far left and right of the map give very similar values. This reduces the effectiveness of this sensor pair, and so the accuracy of the technique.

Throughout testing a DSLR camera was used to identify the presence and size of a crack from the hole and notch on the skin. Prior to loading in the four-point bend test a 4mm crack was visible, as shown in Figure 6 (a).

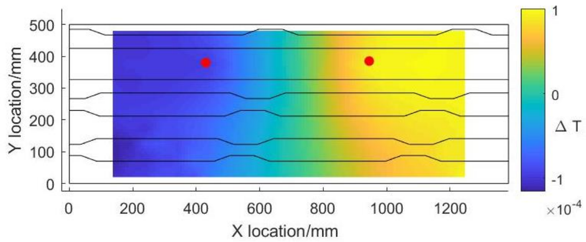

Figure 5. Delta-T map for a sensor pair. Sensors shown a filled circles and stifener edges/edge of panel as lines

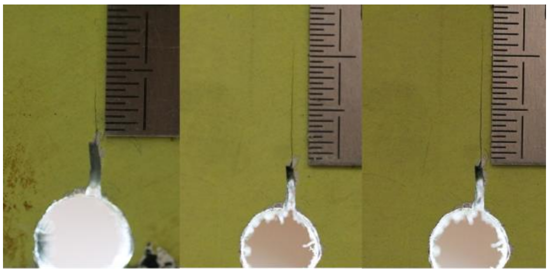

Figure 6. Imaged of the crack in the notch before test 1 (a), before test 15 (b) and after test 15 (c)

A test of interest, that prompted additional examination of the structure, which is covered below, was test 15. Figure 6 (b) and (c) show a 2mm growth in crack occurred during this test, which consisted of 10,000 cycles of 5kN – 80kN at 0.5Hz. A map of the cumulative number of hits accumulated during this test, and located with the Delta-T approach is shown in Figure 7.

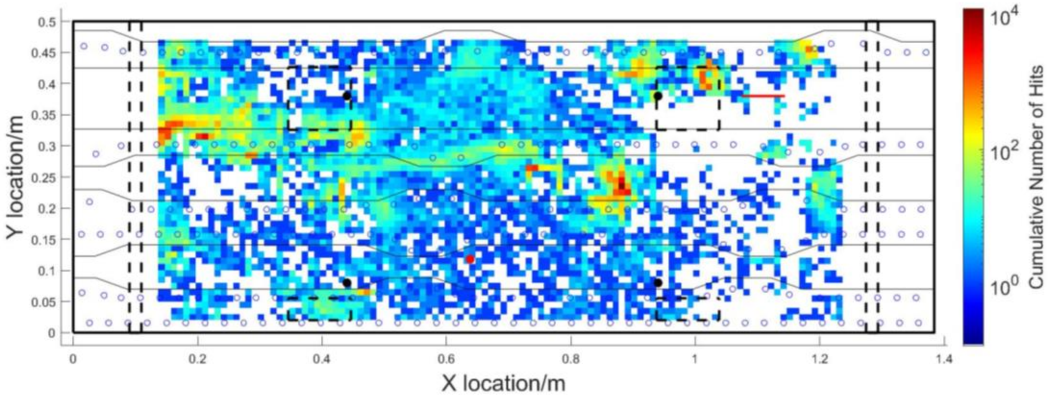

Figure 7. Cumulative AE located within each 10mm squared for Test 15. Circle at x = 0.65, y = 0.1 indicates hole and line at x=1.1, y = 0.4 indicates crack on stiffener. Note scale is logarithmic.

Figure 7 shows the location of the hole and notch, unfortunately there is no cluster of AE located at this point. Instead a major hotspot has been located at x = 0.9m and y =0.25m. Additional hotspots are also present, however the aforementioned has the highest energy.

After test 15, the specimen was thoroughly inspected using dye penetrant spray. No other cracks than from the notch were identified in the skin of the panel. An inspection was then conducted on the other side of the specimen. With visual inspection nothing was detected, however the dye penetrant reviled an 60m crack on one of the stiffeners. This is shown in Figure 8 and its location indicated as a line in Figure 7.

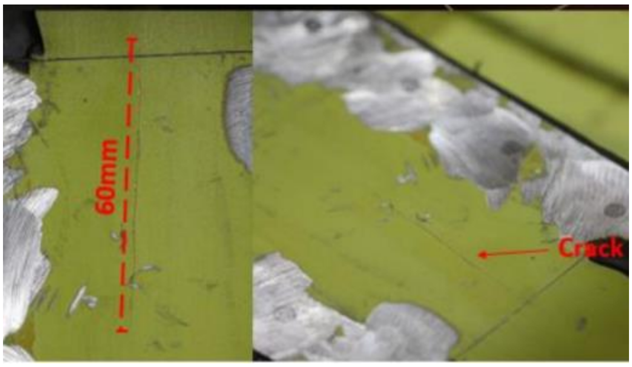

Figure 8. Crack located on stiffener

The 3D nature of this section of stiffener, as well as the fact that it was not mapped, means that location of damage is unlikely to be correct when located with the 2D Delta-T mapping approach. To understand where it would be located, five H-N sources were created every 10mm along the length of the crack. These events were located to the same point as the hotspot in Figure 7, confirming that this hotspot is a result of the crack on the stiffener, shown in Figure 8. This highlights the need for further development of the Delta-T technique for 3D localisation to make it more precise and expand the potential application of the technique.

As the crack on the stiffener had not previously been identified, it was unknown if this was present prior to the start of testing, created in the early size point bend tests or during the 4-point bent test. Further inspection of all the results indicated that AE energy was being located from this area throughout testing, prior to loads reaching 30 kN. It was also found, through visual monitoring of the crack during tests beyond test 15, that crack growth occurred. These findings indicate that it is likely the crack was present prior to the start of testing, with no growth. This means that any AE generated was due to face rubbing, which would be generated in high quantities as the crack is parallel to applied load.

There are numerous reasons why the crack on the stiffener was located, but not the one on the skin. Firstly, unlike on the stiffener crack, little or no rubbing of the crack surfaces is occurring as the load is being applied perpendicular to its growth. Additionally, to minimise movement in the specimen a load was applied continuously, hence the 5-80kN loading cycle; which meant that the crack never fully closed. In real applications, loading on a skin varies much more, with a load being present in a variety of directions, generating greater crack face rubbing.

However, lack of rubbing is not the reason for the system not detecting the AE generated through crack growth. This is attributed to the amplitude of the AE being too low when generated, due to aluminium being a ductile material, and crack growth producing relatively little energy. This low amplitude source is then attenuated when travelling through the structure, further reducing its amplitude when arriving at the sensors. This, combined with the high background noise, and no front-end filtering which could improve detection, meant that it was not detected.

In addition to the AE generated from the crack on the stiffener, Figure 7 shows other hotspots of AE. As no cracks were located at these locations, they are likely to be due to movement/rubbing between the specimen and the test fixtures. This highlights the need for classification of data, to distinguish between damage and background noise.

Overall, the Delta-T mapping approach was shown to be significantly more accurate than the standard TOA method. The successful elements of the test, such as the detection of an unknown crack are positive, however more representative loading is required for future trials, to increase the likelihood that all damage is detected. AE continues to be a promising technique for the monitoring of both in service aircraft and structural testing, however further investigation is required into 3D source location. High data rates and a large quantity of data also highlight the need for front end filtering.

IOP Conf. Series: Materials Science and Engineering 1024 (2021) 012029 doi:10.1088/1757-899X/1024/1/012029

5. Conclusions

This work presents the fatigue testing of an aluminium A320 wing section, monitored using AE. The Delta-T source location technique was shown to be significantly more accurate at locating AE sources in complex structures compared to those used by commercial systems. Two cracks were identified during the testing, one of which purposely created, the other present from the outset, and unknown about. This latter crack was successfully identified by the AE system, with some error due to the 3D nature of the structure. Further work is needed in order to extend the mapping work to such 3D structures.

6. References

Al-Jumaili, S.K., Pearson, M.R., Holford, K.M., Eaton, M.J. and Pullin, R. (2016), “Acoustic emission source location in complex structures using full automatic delta T mapping technique”, Mechanical Systems and Signal Processing, Elsevier, Vol. 72–73, pp. 513–524.

ASTM. (1999), “Standard Guide for Determining the Reproducibility of Acoustic Emission Sensor Response”.

Baxter, M.G., Pullin, R., Holford, K.M. and Evans, S.L. (2007), “Delta T source location for acoustic emission”, Mechanical Systems and Signal Processing, Vol. 21 No. 3, pp. 1512–1520.

Crivelli, D., Guagliano, M. and Monici, A. (2014), “Development of an artificial neural network processing technique for the analysis of damage evolution in pultruded composites with acoustic emission”, Composites Part B: Engineering, Vol. 56 No. Supplement C, pp. 948–959.

Holford, K.M., Eaton, M.J., Hensman, J.J., Pullin, R., Evans, S.L., Dervilis, N. and Worden, K. (2017), “A new methodology for automating acoustic emission detection of metallic fatigue fractures in highly demanding aerospace environments: An overview”, Progress in Aerospace Sciences, Vol. 90, pp. 1–11.

Kaminski-Morrow, D. (2012), “Airbus admits no quick-fix for A380 wing-rib crack issue”, Flightglobal.Com, Flightglobal, FlightGlobal.com.

Lamb, H. (1917), “On Waves in an Elastic Plate”, Proceedings of the Royal Society of London. Series A, Vol. 93 No. 648, pp. 114–128.

McCrory, J.P., Al-Jumaili, S.K., Crivelli, D., Pearson, M.R., Eaton, M.J., Featherston, C.A., Guagliano, M., et al. (2015), “Damage classification in carbon fibre composites using acoustic emission: A comparison of three techniques”, Composites Part B: Engineering, Vol. 68 No. Supplement C, pp. 424–430.

Miller, K.R. and Hill, E.K. (1987), Non-Destructive Testing Handbook; Acoustic Emission Testing, edited by McIntire, R.K.M.P.American Society for Non-Destructive Testing, Vol. VoL 5, American Society of Nondestructive Testing, USA.

Paget, C.A., Atherton, K. and O’Brien, E. (2003), “Triangulation algorithm for damage location in aeronautical composite structures”, Proceedings of the 4th International Workshop on Structural Health Monitoring (F. Chang, Ed.),(Stanford, CA, USA), pp. 363–370.

Pearson, M.R., Eaton, M., Featherston, C., Pullin, R. and Holford, K. (2017), “Improved acoustic emission source location during fatigue and impact events in metallic and composite structures”, Structural Health Monitoring, Vol. 16 No. 4, pp. 382–399.

Rodrigues Vieira, D. and Loures, P.L. (2016), “Maintenance, Repair and Overhaul (MRO) Fundamentals and Strategies: An Aeronautical Industry Overview Holds the research chair in Management of Aeronautical Projects Université du Québec à Trois Rivières-Canada”, International Journal of Computer Applications, Vol. 135 No. 12, pp. 975–8887.

7. Acknowledgments

This work part of the Innovate UK funded project SENTIENT. Further analysis and attendance to the EASN conference was funded though Airbus Endeavr funding, a collaboration between Airbus, the Welsh government, and Cardiff University.